

Adversarial Examples on Discrete Sequences for Beating Whole-Binary Malware Detection

Felix Kreuk, Assi Barak, Shir Aviv-Reuven, Moran Baruch, Benny Pinkas, and Joseph Keshet
Bar-Ilan University
krukfel@biu.ac.il

Abstract

In recent years, deep learning has shown performance breakthroughs in many applications, such as image detection, image segmentation, pose estimation, and speech recognition. It was also applied successfully to malware detection. However, this comes with a major concern: deep networks have been found to be vulnerable to adversarial examples. So far successful attacks have been proved to be very effective especially in the domains of images and speech, where small perturbations to the input signal do not change how it is perceived by humans but greatly affect the classification of the model under attack.

Our goal is to modify a malicious binary so it would be detected as benign while preserving its original functionality. In contrast to images or speech, small modifications to bytes of the binary lead to significant changes in the functionality.

We introduce a novel approach to generating adversarial example for attacking a whole-binary malware detector. We append to the binary file a small section, which contains a selected sequence of bytes that steers the prediction of the network from malicious to be benign with high confidence. We applied this approach to a CNN-based malware detection model and showed extremely high rates of success in the attack.

1 Introduction

Artificial intelligent and deep learning has been recently amongst the most emerging fields in computer science and engineering. Deep learning has been successfully applied to many fields of modern society [27] and specifically has had several breakthroughs in prominent problems such as image classification [25, 17], speech recognition [3], and machine translation [4]. Naturally it is becoming a technology of interest in static malware analysis and detection [42, 7, 37, 40].

In recent years it has been shown that deep networks are vulnerable to attacks by adversarial examples. Adversarial examples are synthetic inputs that are generated by modifying legitimate inputs. In the fields of image processing and speech recognition, modified inputs are considered adversarial when they are indistinguishable by humans from the legitimate examples, and yet they fool state-of-the-art classification systems [15, 32, 26].

Attacks by adversarial examples accentuate the fragility of machine learning in general, and of deep learning in particular [33]. It has triggered an active line of research concerned with understanding the phenomenon [13, 12], and making neural networks more robust [35, 8].

In the domain of malware detection, an adversarial example is a malicious binary file that evades detection while retaining its malicious functionality. More specifically, an adversarial example is a binary file that is generated by modifying an existing malicious binary. While the original file is correctly classified as malicious, its modified version is misclassified as benign, hence evading detection.

Recently, a series of works [21, 16, 19] have shown that adversarial examples cause a catastrophic failure of malware classification systems. Those works assumed a malware detection classifier that was designed with a set of features that were handcrafted and focused, for example, on the PE header data.

Our work is focused on a general and common deep learning architecture called Convolutional Neural Network (CNN). We are interested in attacking modern end-to-end malware detectors [37]. Such detectors are not based on handcrafted features of the input, but rather on the entire *raw binary*. End-to-end deep learning is one of the most important concepts in recent state-of-the-art systems for many tasks.

The goal of this work is to attack an end-to-end malware detector which gets as input a whole binary file. Attacking an end-to-end CNN model has been successfully

done on image detection [6], image segmentation, pose estimation, and speech recognition [9]. In all those domains, a small change in the input (namely in image pixels or in the speech samples) essentially does not change the human perceptual understanding of the input. The situation is entirely different with regards to words in a written language or with bytes in binary files, as changing one word or byte in these types of inputs completely alters the meaning or functionality. We are not aware of an effective attack on deep learning models that are applied to inputs of this latter type.

In short, the contributions of this paper are as follows:

- We show a successful design of an adversarial example attack on a whole-binary malware detector.
- We present a novel attack on discrete input sequences whose “meaning” might be completely changed even by small changes to the input (this is in contrast to attacks on real-valued input vectors such as images or voice).
- We present a new surrogate loss function to effectively achieve this goal.

Organization: This paper is organized as follows. Section 2 gives a background on malware detection and adversarial examples. Section 3 presents related work in deep-learning based malware detection, and adversarial examples applied to this task. In Section 4 we formally set the notations and definitions used throughout the paper. Section 5 introduces the deep learning model and the architecture that is used in this work. Section 6 describes the mechanism behind the generation of adversarial examples, and the new surrogate loss function. Section 7 describes how the functionality of binary files is preserved despite adversarial perturbation. Section 8 reports the results of attacking the malware detection deep learning system utilizing various approaches. We conclude the paper with a discussion in Section 9.

2 Background

Malware detection Malware is a malicious software which upon execution could cause unexpected faulty behavior resulting in information leakage, compromise of the host machine or additional severe negative security outcomes. Malware detection is a cat-and-mouse game between bad-actors and defenders. As malware detection systems introduce new methods, bad-actors constantly introduce methods to detect and evade the defenders.

Signature-based detection is the most basic technique for detecting malware. Signature-based malware detection systems search for file and system-wide indicators that are often named Indicators of Compromise (IOC).

Attackers are well aware of signature-based static analysis. They evade it by using metamorphic and polymorphic techniques in their code, using packers and encryption, and changing their communication techniques. Therefore, signature-based detection is generally considered a wide net that catches the fish we know of but is not an effective means against *unseen malware*.

Malware detection can be based on either *static analysis* or *dynamic analysis*. The static analysis attempts to detect malware without executing the code. In dynamic analysis, a suspicious code is executed in a sandbox, and its dynamic behavior (such as API call sequences) is monitored.

Attackers evade dynamic analysis by attempting to detect execution in a sandbox, for example by detecting that the malware is running in a VM, detecting debuggers, etc. Another drawback of dynamic analysis is that it imposes high computation requirements on the malware detector.

To defend against these evasions, malware detection systems use heuristics such as file and section entropy and additional methods which attempt to classify between malware and benign artifacts. As this is a common setting for learning methods, this leads to a discussion on *machine learning* for malware detection, which we elaborate upon in the following section.

Learning-based malware detection Machine learning and especially deep learning methods are widely used for classification tasks in many fields such as computer vision [25], speech [18] and NLP [29], and typically beat other state-of-the-art algorithms. In the field of binary analysis, research described in [42] and [7] applied recurrent neural network (RNN) on binary files to tackle the problem of function identification and to recover function type signatures from disassembled binary code.

Another domain where similar methods were applied is malware detection, by analyzing n-grams of the bytes file [38], and mining API calls [39, 21]. Those approaches do not work on the entire binary, and seem more fragile to attacks based on slight modifications by the malware author.

There have been attempts to use deep learning as a static analysis mechanism for malware detection. Initial constructions applied a deep learning based analysis to only part of the file. For example, by analyzing the Android manifest [16], by using random projection from the bytes to reduce features [49], or by extracting specific features such as byte entropy histogram, PE imports features, and PE metadata features [40]. However, these techniques do not analyze the whole executable, and might miss relevant information that exists in the code itself, since malware authors may ignore format conventions, and may hide the malicious code in other

areas of the file.

Deep learning on whole-binary executables A recent study by Raff et al. [37] demonstrated a malware detection system named *MalConv*, which is based on end-to-end CNN model. This system is domain-knowledge free. It operates over the entire executable by looking at the raw bytes of the file itself, and builds a neural network model to determine the maliciousness of the file. The experiments in that work processed a raw byte sequence of 1-2MB. This model learns a wider breadth of information types compared to the previous approaches to malware detection. This network is the target of our exploration.

Adversarial examples Although deep neural networks have been shown to outperform other models in the area of classification, it is now evident that such networks can be easily fooled into misclassifying samples, even when the input is perturbed in a very small way and humans still classify it correctly. In the area of image processing this implies that the perturbed image and the original image look the same to any human observer. In the area of speech recognition this is defined by inability of humans to distinguish the variations in the audio [9]. The modified input data is named *adversarial example* as its main purpose is to challenge the original classification.

The difficulty in generating adversarial examples for binary executables There are very few studies related to adversarial examples against deep learning models for malware classification. In [16] it was demonstrated how to generate adversarial examples by adding or removing features from the Android application manifest file. The work in [21] inspected the sequence of API calls made by the inspected code.

To the best of our knowledge, there is no study of adversarial examples with regards to the analysis of the entire binary. The reason for the lack of work in this area might be that the challenges in crafting an adversarial example on executable files are different and more difficult than in other known fields. For example, adversarial examples for image detection decide which pixels to change by calculating the maximum loss and accordingly updating the gradients of the learned model. This is possible since adding very small perturbations to pixels of an image does not affect how humans perceive the image. The case of binary files is inherently different since the files are composed of discrete bytes, and small modifications to the bytes might cause large changes to the functionality.

Adversarial examples of binary files are also different with respect to defining and minimizing the distance of

the adversarial example from the original item. In images the distance must be small and undetectable by humans. In the case of executable files there is no need for the difference from the original file to be small or be undetectable to humans, but there is a new constraint that the functionality of executing the file will remain exactly as before.

3 Related Work

There had been multiple studies in the area of adversarial example generation to fool deep networks. These studies showed that while deep networks can achieve high performance on unknown input, they are vulnerable to small perturbations causing misclassification [13, 6]. Additional studies have described how such adversarial examples can be crafted [20]. Furthermore, Szegedy et al. [45] showed *cross model generalization* where the same adversarial examples could be misclassified by networks trained from scratch with different hyperparameters and *cross training-set generalization* where the same adversarial examples could be misclassified by networks trained from scratch on a different training set. They performed their research on image classification models.

Cisse et al. [9] introduced a novel flexible approach named Houdini for generating adversarial examples specifically tailored for the final performance measure of the task considered. They authors attacked speech recognition, human pose estimation and semantic segmentation systems with a high success rate. Kreuk et al. [24] investigated the generation of adversarial examples for attacking end-to-end neural based speaker verification models, and Carlini et al. [5] showed adversarial attack on a voice command system.

Previous work on adversarial examples for malware detection extracted handcrafted features of binaries and investigated systems that classify files based on these features. We describe here some of the previous work in this field.

Grosse et al. [16] trained a feed-forward neural network on a vector of features extracted from Android APK manifest files. They applied an algorithm for crafting adversarial examples as is done on images in [34], and appended additional features at the end of the manifest. This method achieved misclassification rate of 85% on malicious binaries.

Hu et al. [19] proposed a generative adversarial network (GAN)-based approach which took original samples and output adversarial examples. The work used binary features representing API calls. Then, bogus API calls were simulated by switching binary features when generating adversarial examples.

Xu et al. [48] presented genetic programming techniques to evade malicious PDF detection systems, in order to automatically generate evasive variants. Since the body of a PDF file has a tree-like structure, it is easy to utilize genetic programming to alter and move subtrees to generate new variants. From a small set of test samples they were able to achieve 100% evasion rate by iteratively generating variants that preserve malicious behavior but are classified as benign.

4 Problem Setting

In this section we rigorously formulate the task of malware detection and set the notation for the rest of the paper. A binary input file, whether malicious or benign, is composed of a sequence of bytes. We denote the set of all bytes as $\mathbf{X} \subseteq [0, N - 1]$, where $N = 256$. A binary file is a sequence of L bytes $\mathbf{x} = (x_1, x_2, \dots, x_L)$, where $x_i \in \mathbf{X}$ for all $1 \leq i \leq L$. Note that the length L varies from one binary file to another, thus L is not fixed. We denote by \mathbf{X}^* the set of all finite length sequences, hence $\mathbf{x} \in \mathbf{X}^*$.

The goal of a malware detection system is to classify whether an input binary file is malicious or benign. This system is therefore a function that gets as input a binary file $\mathbf{x} \in \mathbf{X}^*$, and outputs the probability that the binary file \mathbf{x} is malicious. Formally, we denote by $f_\theta : \mathbf{X}^* \rightarrow [0, 1]$ the malware detection function implemented as a neural network with a set of parameters θ .

Given a set of training examples, the parameters θ are found by minimizing the binary negative log-likelihood loss function. Each example in the training set is a tuple (\mathbf{x}, y) of a binary file $\mathbf{x} \in \mathbf{X}$ and a label $y \in \{0, 1\}$ indicating whether the binary file \mathbf{x} is benign or malicious. If the output of $f_\theta(\mathbf{x})$ is greater than 0.5 then the prediction is considered as 1 or *malicious*, otherwise the prediction is considered as 0 or *benign*.

The goal of this work is to modify a binary file, while preserving its functionality, in order for it to be misclassified by the neural network. More specifically, given a malicious file, which is correctly classified as *malware*, we would like to slightly modify it, while maintaining its original functionality, so that it will be classified as *benign*. Formally, denote by $\tilde{\mathbf{x}}$ the modified version of the malicious file \mathbf{x} . Note that if \mathbf{x} is classified as *malware*, $f_\theta(\mathbf{x}) > 0.5$, then we would like to design $\tilde{\mathbf{x}}$ such that $f_\theta(\tilde{\mathbf{x}}) < 0.5$, and the prediction is *benign*.

5 Learning Apparatus

In this section we describe the training procedure of neural networks (NNs). Recall that a neural network is a function $f_\theta : \mathbf{X}^* \rightarrow [0, 1]$ parameterized by θ , where \mathbf{X}^* is the domain of all finite length binary files. We assume

that a binary file \mathbf{x} and its corresponding label $y \in \{0, 1\}$ are drawn from a fixed but unknown distribution ρ . We denote by $\hat{y}_\theta \in \{0, 1\}$ the predicted label by the neural network:

$$\hat{y}_\theta(\mathbf{x}) = \begin{cases} 0 & \text{if } f_\theta(\mathbf{x}) \geq 0.5 \\ 1 & \text{if } f_\theta(\mathbf{x}) < 0.5 \end{cases} \quad (1)$$

In general, each task defines its own measure of performance [1, 2]. In the task of malware detection, the performance of the system is evaluated by the *0-1 loss function* defined as being 1 if the true label y is not equal to the predicted label \hat{y} , and 0 otherwise. That is

$$\ell(y, \hat{y}) = \mathbb{1}[y \neq \hat{y}] = \begin{cases} 0 & \text{if } y = \hat{y} \\ 1 & \text{if } y \neq \hat{y} \end{cases}, \quad (2)$$

where $\mathbb{1}[\pi]$ is the indicator function over the predicate π . The goal of training is to find the parameters θ that minimize the expectation of the desired loss function [22]

$$\theta^* = \arg \min_{\theta} \mathbb{E}_{(\mathbf{x}, y) \sim \rho} [\ell(y, \hat{y}_\theta(\mathbf{x}))], \quad (3)$$

or specifically

$$\theta^* = \arg \min_{\theta} \mathbb{E}_{(\mathbf{x}, y) \sim \rho} [\mathbb{1}[y \neq \hat{y}_\theta(\mathbf{x})]]. \quad (4)$$

Unfortunately there are two caveats in the above formalization: (i) the probability density function ρ is unknown; and (ii) the indicator function cannot be minimized directly as it is a combinatorial quantity.

The common practice in machine learning is to replace the expectation with an average over a training set of examples drawn from the distribution ρ , and replace the desired loss function, i.e., the 0-1 loss, with a surrogate loss function denoted as $\bar{\ell}(\mathbf{x}, y; \theta)$, for an example (\mathbf{x}, y) and parameters θ . Most often, the surrogate loss function used in training binary NN is the negative log-likelihood, defined as

$$\bar{\ell}(\mathbf{x}, y; \theta) = -y \log(f_\theta(\mathbf{x})) - (1 - y) \log(1 - f_\theta(\mathbf{x})). \quad (5)$$

Overall, the parameters θ are found by solving the following optimization problem:

$$\theta^* = \arg \min_{\theta} \frac{1}{m} \sum_{i=1}^m \bar{\ell}(\mathbf{x}_i, y_i; \theta), \quad (6)$$

where $S = \{(\mathbf{x}_i, y_i)\}_{i=1}^m$ is the training set of m examples.

The above optimization problem is solved using *Stochastic Gradient Descent* or similar gradient-based algorithms [11, 46, 23]. These algorithms offer an iterative method for minimizing an objective function, in our case, the loss function $\bar{\ell}$. This is achieved by iteratively updating the set of parameters θ :

$$\theta \leftarrow \theta - \eta \cdot \nabla_{\theta} \bar{\ell}(\mathbf{x}, y; \theta) \quad (7)$$

Where η is the learning-rate.

In this paper, we exemplify our ideas using Convolutional Neural Networks (CNNs). CNNs have shown state-of-the-art results in many tasks and applications [47, 17] and specifically in the task of malware detection [37].

5.1 Convolutional neural networks

Convolutional neural networks are a class of deep neural networks. In a convolutional layer a *filter* is convolved around an input vector, yielding an output referred to as a *feature map*. Every coordinate in the feature map can be interpreted as representation of a small region in the input.

CNNs have some desirable properties: (i) the nature of convolving a filter around an input vector yields a model that is *shift-invariant*. In other words, it is agnostic to the spatial location of the features and is specialized at the pattern recognition; (ii) Each filter is replicated across the entire input. The replicated units share the same parameters. This drastically reduces the amount of learned parameters, resulting in better generalization, faster convergence and lower risk of over-fitting the data; and (iii) CNNs exploit spatially local correlation by having its layers locally-connected in contrast to fully-connected networks, and thus resulting in a feature map that is highly spatially correlated to the input.

The feature map is often passed through a non-linear activation function before being down-sampled. Down-sampling is achieved by a concept called *pooling*. There are several non-linear ways to perform pooling, the most common being *max-pooling*. It partitions the input into non-overlapping fixed-size regions, each region is represented by its max value. Pooling layers progressively reduce the spatial size of their input, hence reducing the amount of parameters and computation needed.

Before turning to describe the neural network architecture used in this work, we describe how a binary file is meaningfully represented to the network.

5.2 Representations

Recall that a binary file \mathbf{x} is a sequence of discrete values (bytes). Since the actual values in the sequence are arbitrary, a neural network cannot find meaningful semantic concepts between different values. A common approach to representing a discrete variable is to use a *one-hot* representation. In our case, each element in the sequence, x_i where $1 \leq i \leq L$, represents a discrete variable, which belongs to the discrete set $\mathbf{X} \subseteq [0, N - 1]$. The one-hot representation of the element x_i whose particular value is $q \in \mathbf{X}$ is defined as a vector $\mathbf{x}^{\text{one-hot}} \in \{0, 1\}^N$ where

all its values are 0 except for the value at the q -th index which is set to 1. That is

$$x_j^{\text{one-hot}} = \begin{cases} 1 & \text{if } j = q \\ 0 & \text{if } j \neq q \end{cases}, \quad (8)$$

for $1 \leq j \leq |\mathbf{X}|$. Such a representation allows the network to multiply each element with a different weight and find a relevant relationship between similar elements. The downside of this representation is two-fold: (i) it is highly sparse, and (ii) all bytes have equal distance from each other, regardless of their semantic distance.

In order to solve the above caveats the one-hot representation is often coupled with a dense representation called an *embedding*. An embedding is a mapping of the one-hot vector to a real-valued vector space denoted as $\mathbf{Z} \subseteq \mathbb{R}^D$, where D is the embedding size (in our setting we used $D = 8$). In this vector space, each embedding vector represents a byte and its contextual information, and embedding vectors which are close to each other correspond to bytes which share similar contexts and semantic meaning. Overall each binary file is represented in the embedded vector space as a sequence of vectors $\mathbf{z} = (\mathbf{z}_1, \mathbf{z}_2, \dots, \mathbf{z}_L)$, where $\mathbf{z}_i \in \mathbf{Z}$ for all $1 \leq i \leq L$.

We define h_θ to be a function that maps from the domain of one-hot vectors to the domain of the real valued vector space \mathbf{Z} . A common way to implement such function is by a *look-up table* $\mathbf{M} \in \mathbb{R}^{N \times D}$. In particular, the function f_θ is considered as a composition of h_θ and the function g_θ , where $g_\theta : \mathbf{Z} \rightarrow [0, 1]$. That is, $f_\theta = g_\theta \circ h_\theta$. The mapping of the one-hot vectors to the embedding space is usually learned as part of the training procedure [14], or separately as in [31, 36].

5.3 Model architecture

In this section, we describe the network architecture used as our malware detection function [37], which is schematically depicted in Figure 1. Recall that an input file \mathbf{x} is a sequence of discrete bytes. It is the input to the embedding function h_θ which maps it to the embedding vector \mathbf{z} . The embedding \mathbf{z} is then fed into two convolutional layers, one of which is sigmoid-activated. The corresponding outputs of these layers are multiplied element-wise [10]. This output is then passed to a *temporal max pooling* layer, which is a special case of *max pooling*, where the region that is being processed is the entire feature map. The pooling layer reduces all variable-length sequences to a fixed size. The sequence representation is then fed to a fully-connected layer, reducing it to the desired output size.

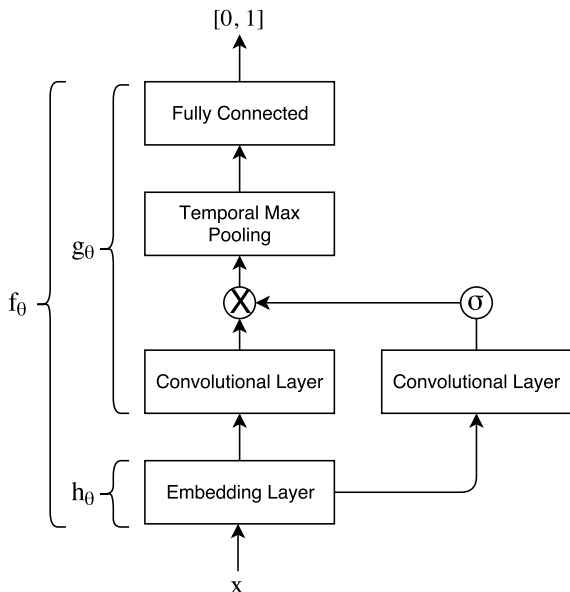


Figure 1: deep network model for malware detection. The architecture is based on [37].

6 Generating Adversarial Examples

In this section we present the generation of adversarial examples. Our goal is to modify a binary file such that it will be misclassified by the network, while preserving its original functionality. In particular, if the binary file is malicious, and detected by the network as such, we would like to slightly modify it so it will be classified as *benign*, but will still function as malware. This section presents how to create an adversarial example for a discrete domain, while next section presents how we apply the method so as to keep the functionality of the binary file.

As discussed in Section 5.2, the representation of the binary file as a sequence of bytes is arbitrary, hence the neural network cannot effectively work in this space, nor an adversarial example can be effectively generated. Generating adversarial examples is done by adding small perturbations to the original example which are in the direction of increasing/decreasing gradient. Such methods fail to work because perturbing one-hot vectors results in a vector that is no longer in the one-hot vector space. We start this section by presenting how to create adversarial examples in the *embedding* domain. Then we present how to reconstruct a new binary file from the modification done in the embedding space.

6.1 Generating adversarial examples for a discrete input set

Given an input binary file that is represented in the embedded domain $\mathbf{z} \in \mathbf{Z}^*$, an adversarial example is a perturbed version of the original pattern

$$\tilde{\mathbf{z}} = \mathbf{z} + \delta, \quad (9)$$

where $\delta \in \mathbf{Z}^*$ is additive perturbations generated such that the functionality of \mathbf{z} is preserved, but causes the network to predict an incorrect label.

We assume that the network g_θ was trained and the parameters θ were fixed. A target adversarial example is generated by solving the following optimization problem

$$\tilde{\mathbf{z}} = \arg \min_{\tilde{\mathbf{z}}: \|\tilde{\mathbf{z}} - \mathbf{z}\|_p \leq \epsilon} \bar{\ell}(\tilde{\mathbf{z}}, y; \theta), \quad (10)$$

where y is the desired target label (*benign* in our case), ϵ represents the strength of the adversary, and p is the norm value. In words, we would like to minimize the loss function between the prediction of g_θ on the adversarial example and the target label under the constraint that the adversarial example is similar to the original example in p -norm.

Assuming the loss function $\bar{\ell}$ is differentiable, the authors of [41] proposed to take the first order Taylor expansion of $\mathbf{x} \mapsto \bar{\ell}(\tilde{\mathbf{z}}, y; \theta)$ to compute δ by solving the following problem:

$$\tilde{\mathbf{z}} = \arg \min_{\tilde{\mathbf{z}}: \|\tilde{\mathbf{z}} - \mathbf{z}\|_p \leq \epsilon} (\nabla_{\tilde{\mathbf{z}}} \bar{\ell}(\tilde{\mathbf{z}}, y; \theta))^T (\tilde{\mathbf{z}} - \mathbf{z}) \quad (11)$$

When using the max norm, $p = \infty$, the solution to the optimization problem is

$$\tilde{\mathbf{z}} = \mathbf{z} + \epsilon \cdot \text{sign}(\nabla_{\tilde{\mathbf{z}}} \bar{\ell}(\tilde{\mathbf{z}}, y; \theta)), \quad (12)$$

which corresponds to the *fast gradient sign method* (FGSM) proposed in [20]. When choosing $p = 2$ we get

$$\tilde{\mathbf{z}} = \mathbf{z} + \epsilon \cdot \nabla_{\tilde{\mathbf{z}}} \bar{\ell}(\tilde{\mathbf{z}}, y; \theta). \quad (13)$$

Recall that in during training a scaled version of the loss is added to the parameters as in Equation (7). Similarly, in generating adversarial examples, a scaled version of the gradient (or its sign) is added to an example. Optionally, one can perform more iterations of these steps using a smaller norm. This more involved strategy has several variants [32].

After the adversarial example of $\tilde{\mathbf{z}}$ was crafted, we need to reconstruct the new binary file $\tilde{\mathbf{x}}$. The most straightforward approach is to map each \mathbf{z}_i to its closest neighbor in the embedding matrix \mathbf{M} , which is a lookup table that assigns a vector in \mathbf{Z} to each input in \mathbf{X} . While this approach works most of the time, we can further enhance it to have higher success rates.

Algorithm 1: Adversarial Examples Generation

Data: A binary file \mathbf{x} , target label y
 $\mathbf{x}^{\text{suffix}} \sim \mathbf{U}(0, N-1)^k$
 $\mathbf{z}^{\text{suffix}} \leftarrow \mathbf{M}(\mathbf{x}^{\text{suffix}})$
 $\mathbf{z} \leftarrow \mathbf{M}(\mathbf{x})$
// generate adversarial in the embedding domain
 $\tilde{\mathbf{z}}^{\text{suffix}} \leftarrow \mathbf{z}^{\text{suffix}}$
 $\tilde{\mathbf{z}}^{\text{new}} \leftarrow \mathbf{z} \oplus \tilde{\mathbf{z}}^{\text{suffix}}$
while $g_\theta(\tilde{\mathbf{z}}^{\text{new}}) > 0.5$ **do**
 $\tilde{\mathbf{z}}^{\text{suffix}} \leftarrow \tilde{\mathbf{z}}^{\text{suffix}} + \varepsilon \cdot \text{sign}\left(\nabla_{\mathbf{z}} \bar{\ell}^*(\tilde{\mathbf{z}}^{\text{new}}, y; \theta)\right)$
 $\tilde{\mathbf{z}}^{\text{new}} \leftarrow \mathbf{z} \oplus \tilde{\mathbf{z}}^{\text{suffix}}$
end
// reconstruct the new binary file
for $i \leftarrow 0$ **to** L **do**
 $\tilde{\mathbf{x}}_i^{\text{new}} \leftarrow \arg \min_j d(\tilde{\mathbf{z}}_i^{\text{new}}, \mathbf{M}_j)$
end
return $\tilde{\mathbf{x}}^{\text{new}}$

6.2 Enhancing reconstruction

In this subsection we present a novel loss function that enforces the modifications in the embedding space to be such that they will allow a better reconstruction of the binary file. We found out that reconstructing bytes from the perturbed embeddings in \mathbf{Z}^* is often not trivial. In some cases, the perturbed embeddings have lost resemblance to embeddings in the lookup table \mathbf{M} that represents the mapping between bytes to embeddings. Hence, reconstruction from the perturbed embeddings to bytes is no longer sensible. In order to allow better reconstruction, we propose to add a new term to the loss function that imposes the perturbation in \mathbf{Z} will be close to row in the embedding matrix \mathbf{M} .

Denote by $d: \mathbf{Z} \times \mathbf{Z} \rightarrow \mathbb{R}_+$ a distance function, which assigns a low positive number if two embeddings in \mathbf{Z} are close and a high positive number otherwise. Note that $\bar{\ell}$ is the negative log-likelihood loss. To resolve failed reconstruction cases, we propose a new combined surrogate loss function $\bar{\ell}^*(\mathbf{z}, y; \theta)$ defined as:

$$\bar{\ell}^*(\mathbf{z}, y; \theta) = \alpha \bar{\ell}(\mathbf{z}, y; \theta) + (1 - \alpha) \sum_{i=1}^L \min_j d(\mathbf{z}_i, \mathbf{M}_j), \quad (14)$$

where $\alpha \in [0, 1]$ is parameter that weights each loss function, and $\mathbf{M}_j \in \mathbf{Z}$ is the j -th row in the lookup embedding matrix \mathbf{M} . In words, the new loss $\bar{\ell}^*$ is a linear interpolation of 2 terms. The first is the categorical loss, namely the negative log-likelihood loss. The second term reflects the distance of the generated adversarial embeddings from the actual embeddings in \mathbf{M} , this term steer the solution so that the generated adversarial embeddings are reconstructible.

The *min* function in Equation (14) is not differentiable.

We replace it with the sum over all elements, to get an upper-bound to the *min* function. The new loss can be written as follows

$$\bar{\ell}^*(\mathbf{z}, y; \theta) = \alpha \bar{\ell}(\mathbf{z}, y; \theta) + (1 - \alpha) \sum_{i=1}^L \sum_{j=1}^N d(\mathbf{z}_i, \mathbf{M}_j). \quad (15)$$

To generate adversarial examples in the embedding domain we plug Equation 15 into the generation procedure described in Equation (12). Upon successfully crafting the adversarial example $\tilde{\mathbf{z}}$, we reconstruct the new binary file $\tilde{\mathbf{x}}$ as described in Section 6.1

7 Preserving Functionality

So far we have discussed how to modify the embedding vector and reconstruct a modified binary file. However, utilizing this approach directly might not preserve the binary file original functionality as the changes could affect the whole file. Instead, we propose to create a new section with the payload bytes and set a flag indicating it includes initialized readable data. We perturb only this section when crafting the adversarial example. This section can be appended to the original binary file. Alternatively, the crafted section can be added at contingent unused bytes in data and resource sections. Either of the approaches described above would not cause any functionality changes as the perturbed data is inserted at non-executable code sections. In this paper we are focused on the former option of appending a new section and defer the latter option to future work.

We generate adversarial examples using the technique depicted in Algorithm 1 and detailed here. We append a uniformly random sequence of bytes with a length of k , $\mathbf{x}^{\text{suffix}} \in \mathbf{X}^k$, to the original binary file \mathbf{x} . We then embed the new binary $\mathbf{x}^{\text{new}} = \mathbf{x} \oplus \mathbf{x}^{\text{suffix}}$, to get $\mathbf{z}^{\text{new}} = \mathbf{z} \oplus \mathbf{z}^{\text{suffix}}$. Next, the algorithm iteratively perturbs the appended segment $\mathbf{z}^{\text{suffix}}$ and stops when g_θ mis-classifies it. By perturbing only the appended segment, we ensure that \mathbf{z} is kept intact and the functionality of \mathbf{x} is preserved. The result is a file \mathbf{x}^{new} that behaves identically to \mathbf{x} but evades detection by g_θ .

8 Experimental Results

In this section, we present a series of experiments where we show that the attack on a whole-binary malware detector is statistically successful using our proposed method.

The setting of the experiments was similar in all our experiments. We represented binary files as described in Section 4 and trained a malware detector model on that representation in a similar way as described in [37]. We

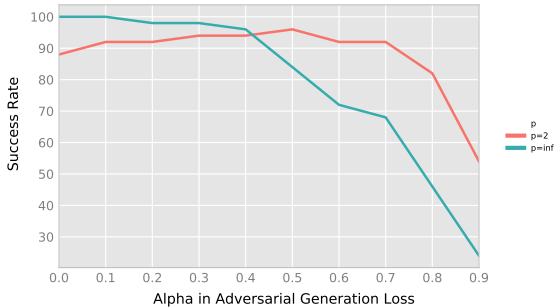


Figure 2: Successful attack rate as function of α for $p = 2$ and $p = \infty$. Success rate of 100% was achieved for $p = \infty$ at α equals either 0 or 0.1.

generated adversarial examples by adding perturbations in the embedding vector space, and then reconstructed new binary files from the adversarial example. We now describe the experimental setting and results in detail.

8.1 Dataset

We evaluated the effectiveness of our method using a dataset for the task of malware detection. Two disjoint sets of files were used. The first set is a collection of benign binary files that was collected as follows. We deployed a fresh Windows 8.1 32-bit image and installed additional software from over 50 vendors using *ninite* [44]. Using files from multiple vendors is essential to avoid learning to recognize the files as associated with a specific vendor (see [37]). We then collected all images (exe or dll) with size 32KB or greater and ignored small resource dlls. This resulted in 7,150 files, which were labeled as *benign*.

The second set is a collection of 10,866 malicious binary files (Win32 PE files) from 9 different malware families: *Ramnit*, *Lollipop*, *Kelihos* (2 classes), *Vundo*, *Simda*, *Tracur* (a.k.a, *Ramnit*), *Gatak*, and *Obfuscator.ACY* (a.k.a *Zbot*). They were taken from *Microsoft Kaggle 2015 dataset*¹ [30]. These files were labeled as *malicious*.

Note that both benign and malicious files are represented as a sequence of bytes from offset 4096, that is, PE Header removed.

8.2 A white-box attack

In the setting of a white-box attack, we assume that the adversary has access to the internals of the model to be attacked. In other words, the attacker has complete knowledge and control of the network and can access the

¹We are grateful to Microsoft for allowing us to use the data for research purposes.

p -norm	Evasion rate	Benign confidence
$p = 2$	88%	0.86
$p = \infty$	100%	0.99

Table 1: Baseline experiment for $\alpha = 0$. The first column is the success rate of attacks, and the second column is the average confidence of class *benign*.

networks’ gradients. An adversary can use these gradients to perturb the original input to become adversarial. The adversarial examples were crafted directly on the inputs that were fed to the network.

We trained a CNN end-to-end malware detector [37] until it reached a classification accuracy of 98% on a validation set. This corresponded to accuracy of 97% on the test set.

Two methods were used to create adversarial examples. The first method was an attempt to modify the instructions in the binary code by employing code obfuscation techniques to create metamorphic variations [28]. Those techniques do not change the functionality of the binary. Unfortunately, we found out that none of the resulted metamorphic variations was misclassified by our CNN malware detector.

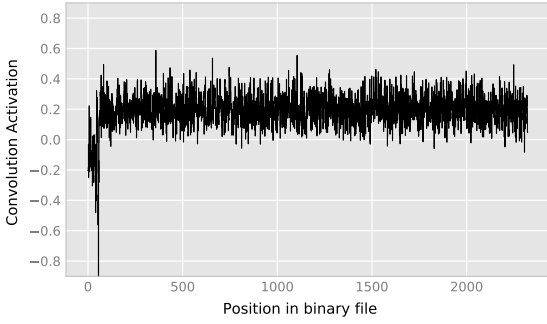
We, hence, continued with a second method where we appended to the binary file a section denoted as $\mathbf{x}^{\text{suffix}}$ that was initiated uniformly at random. Then we generated adversarial examples on the appended section $\mathbf{x}^{\text{suffix}}$ using the iterative FGSM, $p = \infty$, as described in Equation (12), and using $p = 2$ as described in Equation (13). We evaluated the effectiveness of the attack on 100 files picked at random from the test part of the dataset. We checked the success rate of the attack as a function of the parameter α for each of the value of p .

8.3 Detection evasion

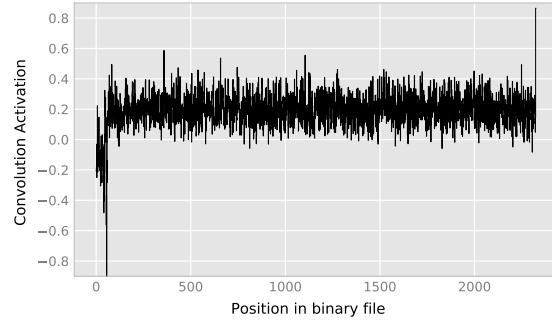
The goal of the of this set of experiments is to modify a malicious binary file such that it would be detected as *benign*. As baseline for all experiments we use a value of $\alpha = 0$. This is the case where only a categorical loss (negative log likelihood loss) is used to generate adversarial examples.

The success of the attack was evaluated using two metrics: (i) precision of successful attacks, i.e., percentage of files for which the classifier confidence in the benign class was above 0.5; and (ii) the average confidence of the class *benign*.

In Table 1 we present the success rate for $p = 2$, and $p = \infty$. It can be seen that we reached a highly successful rate in evading detection. For $p = 2$, we believed that the unsuccessful attacks were due to poor reconstruction:

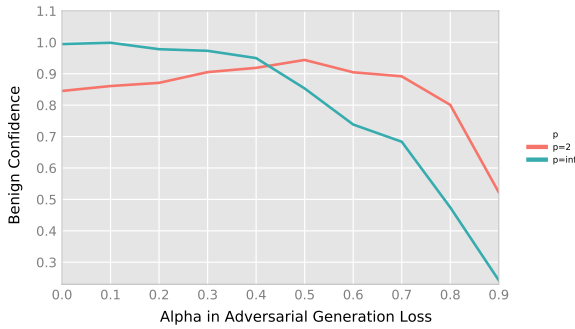


(a) Average convolution activation across 128 filters in original binary file.

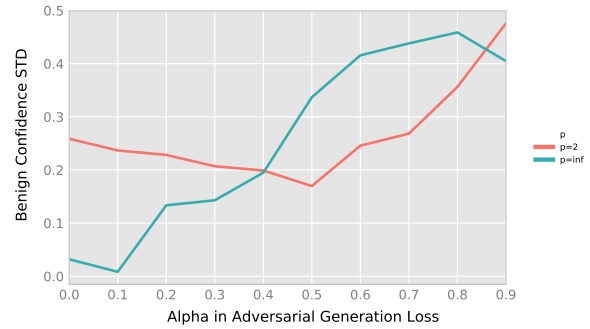


(b) Average convolution activation across 128 filters in adversarial binary file.

Figure 3: "Attention shift" demonstrated in convolutional activations [43]. The adversarial suffix has higher activations on average than the rest of the file, essentially suppressing the rest of the malicious file due to temporal max-pooling.



(a) Average of the confidence.



(b) Standard deviation of the confidence.

Figure 4: The confidence of the class *benign* as a function of the weighting parameter α . The red and cyan lines present the confidence for $p = 2$ and $p = \infty$, respectively.

the embeddings were perturbed to a point where their reconstruction to bytes was no longer sensible, since the perturbed embeddings could not be associated with the fixed embeddings in the lookup matrix \mathbf{M} . To further improve the success rate of the attack for $p = 2$, we integrated the new loss function in crafting of the adversarial examples.

Recall that the parameter α in Equation (15) weights the categorical loss and the embedding-similarity loss, where $\alpha = 0$ means only the categorical loss active and, both the other hand, $\alpha = 1$ means only the similarity-embedding loss active. In Figure 2 we show the success rate of the attack as a function of α for $p = 2$ and $p = \infty$. The highest success rate for $p = 2$ was 95% and reached at $\alpha = 0.5$, while the highest success rate for $p = \infty$ was 100% and reached at α equals 0 and 0.1.

It was shown the adversarial examples shift the attention of neural networks, and CNN in particular [43]. We

present how the adversarial examples shifted the attention of the convolutional network towards the synthetically added suffix. In Figure 3 we shows the activation of the network along the position in a specific binary file (Figure 3-a) and after adding the adversarial suffix to it (Figure 3-b). Recall that in our architecture of a CNN, a temporal-max-pooling operation is performed after the convolution. It is clearly seen that for the adversarial example (Figure 3-b) the maximum was achieved at the suffix, essentially acting as a "distraction" to the malicious payload.

We now turn to discuss the confidence of the network for the adversarial examples. Figure 4 presents the confidence of the class *benign* as a function of the weight α for $p = 2$ and $p = \infty$. We presented both (a) the average and (b) the standard deviation of the confidence. We can see that the highest value of confidences for both values of p matches success rates in Figure 2.

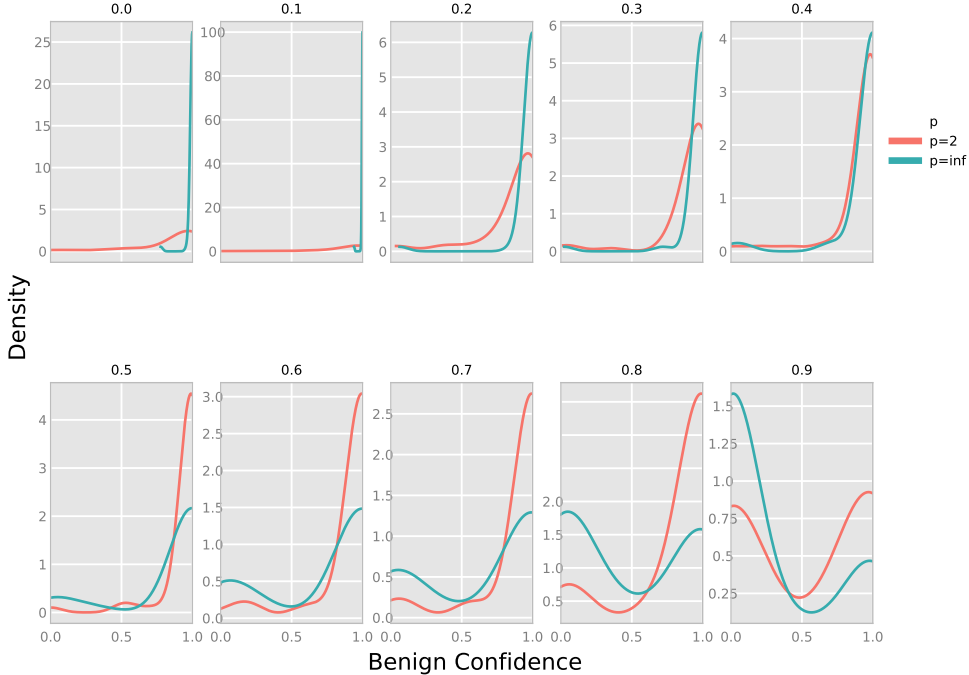


Figure 5: Density functions of benign confidence as function of α . The x axis is the classifier’s benign confidence. Different plots represent different α values.

Interestingly, the standard deviation is the lowest for the values of α that achieves the highest success rate and confidence. While for $p = \infty$ two values of α , 0 and 0.1, achieved 100% success rate, the value $\alpha = 0.1$ has a higher confidence and has a lower standard deviation.

In order to better understand the behavior of the network under the attack, we present density graphs for each value of α and for each p . These graphs shows the distribution of confidence of the class *benign* for each adversarial example. We see how the increase of α corresponds to bigger concentrations around 1. The maximum of the distribution corresponds to the values of α in the previous figures: for $p = 2$ we see that the density is maximized for $\alpha = 0.5$, while for $p = \infty$ the density is extremely picky for $\alpha = 0.1$.

8.4 False alarms

Additionally, experiments were conducted on benign files. We have tested three setups: (i) permuting entire benign files using metamorphism; (ii) permuting the text section of benign files using metamorphism; and (iii) appending random bytes as a new data section to benign files. (i) and (ii) resulted in no change in the classifier’s decision, which remained *benign*. In (i) the new suffix

shifted the classifier’s decision to *malicious* in 100% of our experiments.

9 Discussion and Future Work

In this paper, we demonstrated how to generate adversarial examples to fool a deep neural network for misclassifying malware binaries as benign. Although the network we attacked was found to be robust against adding random data and metamorphic changes in code segments, our approach of appending a section to the binary file and modifying that part only, showed the network was vulnerable to adversarial attacks.

Often an adversarial example that is crafted to deceive model A also deceives model B, even when model B has a different architecture than that of model A (see [9] and the references therein). This phenomenon is called *cross-model* attack. When model B was trained on a different dataset than model A, this is called *cross-dataset* attack. Hence, adversarial examples pose a great security risk even when the attacker does not have access to the model. Our attack method heavily relies on the learned embeddings of the model, which can hinder the transferability of adversarial examples to models with different byte embeddings. In future work, we strive to over-

come this limitation to produce more generic attacks. We will also try to demonstrate cross-dataset attacks on additional datasets, and on a variety of architectures.

Deep learning has shown great breakthroughs in recent years. It seems critical to revisit the evaluation process of deep learning, especially in the case of security sensitive domains in general, and for malware detection in particular.

References

- [1] ADI, Y., AND KESHET, J. Structed: risk minimization in structured prediction. *The Journal of Machine Learning Research* 17, 1 (2016), 2282–2286.
- [2] ADI, Y., KESHET, J., CIBELLI, E., GUSTAFSON, E., CLOPPER, C., AND GOLDRICK, M. Automatic measurement of vowel duration via structured prediction. *The Journal of the Acoustical Society of America* 140, 6 (2016), 4517–4527.
- [3] AMODEI, D., ANANTHANARAYANAN, S., ANUBHAI, R., BAI, J., BATTENBERG, E., CASE, C., CASPER, J., CATANZARO, B., CHENG, Q., CHEN, G., ET AL. Deep speech 2: End-to-end speech recognition in english and mandarin. In *International Conference on Machine Learning* (2016), pp. 173–182.
- [4] BAHDANAU, D., CHO, K., AND BENGIO, Y. Neural machine translation by jointly learning to align and translate. *arXiv preprint arXiv:1409.0473* (2014).
- [5] CARLINI, N., MISHRA, P., VAIDYA, T., ZHANG, Y., SHERR, M., SHIELDS, C., WAGNER, D., AND ZHOU, W. Hidden voice commands. In *25th USENIX Security Symposium (USENIX Security 16)* (Austin, TX, 2016), USENIX Association, pp. 513–530.
- [6] CARLINI, N., AND WAGNER, D. Towards evaluating the robustness of neural networks. In *Security and Privacy (SP), 2017 IEEE Symposium on* (2017), IEEE, pp. 39–57.
- [7] CHUA, Z. L., SHEN, S., SAXENA, P., AND LIANG, Z. Neural nets can learn function type signatures from binaries. In *26th USENIX Security Symposium (USENIX Security 17)* (Vancouver, BC, 2017), USENIX Association, pp. 99–116.
- [8] CISSE, M., BOJANOWSKI, P., GRAVE, E., DAUPHIN, Y., AND USUNIER, N. Parseval networks: Improving robustness to adversarial examples. In *International Conference on Machine Learning* (2017), pp. 854–863.
- [9] CISSE, M. M., ADI, Y., NEVEROVA, N., AND KESHET, J. Houdini: Fooling deep structured visual and speech recognition models with adversarial examples. In *Advances in Neural Information Processing Systems 30*, I. Guyon, U. V. Luxburg, S. Bengio, H. Wallach, R. Fergus, S. Vishwanathan, and R. Garnett, Eds. Curran Associates, Inc., 2017, pp. 6980–6990.
- [10] DAUPHIN, Y. N., FAN, A., AULI, M., AND GRANGIER, D. Language modeling with gated convolutional networks. *arXiv preprint arXiv:1612.08083* (2016).
- [11] DUCHI, J., HAZAN, E., AND SINGER, Y. Adaptive subgradient methods for online learning and stochastic optimization. *Journal of Machine Learning Research* 12, Jul (2011), 2121–2159.
- [12] FAWZI, A., FAWZI, O., AND FROSSARD, P. Analysis of classifiers robustness to adversarial perturbations. *Machine Learning* (2015), 1–28.
- [13] FAWZI, A., FAWZI, O., AND FROSSARD, P. Analysis of classifiers’ robustness to adversarial perturbations. *Machine Learning* (Aug 2017).
- [14] GOLDBERG, Y. Neural network methods for natural language processing. *Synthesis Lectures on Human Language Technologies* 10, 1 (2017), 49.
- [15] GOODFELLOW, I. J., SHLENS, J., AND SZEGEDY, C. Explaining and harnessing adversarial examples. *arXiv preprint arXiv:1412.6572* (2014).
- [16] GROSSE, K., PAPERNOT, N., MANOHARAN, P., BACKES, M., AND MCDANIEL, P. D. Adversarial examples for malware detection. In *Computer Security - ESORICS 2017 - 22nd European Symposium on Research in Computer Security, Oslo, Norway, September 11-15, 2017, Proceedings, Part II* (2017), S. N. Foley, D. Gollmann, and E. Snekkenes, Eds., vol. 10493 of *Lecture Notes in Computer Science*, Springer, pp. 62–79.
- [17] HE, K., ZHANG, X., REN, S., AND SUN, J. Deep residual learning for image recognition. In *Proceedings of the IEEE conference on computer vision and pattern recognition* (2016), pp. 770–778.
- [18] HINTON, G., DENG, L., YU, D., DAHL, G., RAHMAN MOHAMED, A., JAITLY, N., SENIOR, A., VANHOUCHE, V., NGUYEN, P., SAINATH, T., AND KINGSBURY, B. Deep neural networks for acoustic modeling in speech recognition. *Signal Processing Magazine* (2012).
- [19] HU, W., AND TAN, Y. Black-box attacks against rnn based malware detection algorithms. *arXiv preprint arXiv:1705.08131* (2017).
- [20] IAN J GOODFELLOW, JONATHON SHLENS, C. S. Explaining and harnessing adversarial examples. ICLR.
- [21] ISHAI ROSENBERG, ASAF SHABTAI, L. R., AND ELOVICI, Y. Generic black-box end-to-end attack against rnns and other API calls based malware classifiers. *CoRR abs/1707.05970* (2017).
- [22] KESHET, J. Optimizing the measure of performance in structured prediction. In *Advanced Structured Prediction*, S. Nowozin, P. V. Gehler, J. Jancsary, and C. H. Lampert, Eds. The MIT Press, 2014.
- [23] KINGMA, D. P., AND BA, J. Adam: A method for stochastic optimization. *arXiv preprint arXiv:1412.6980* (2014).
- [24] KREUK, F., ADI, Y., CISSE, M., AND KESHET, J. Fooling end-to-end speaker verification by adversarial examples. In *ICASSP* (2018).
- [25] KRIZHEVSKY, A., SUTSKEVER, I., AND HINTON, G. E. Imagenet classification with deep convolutional neural networks. In *Advances in Neural Information Processing Systems 25*, F. Pereira, C. J. C. Burges, L. Bottou, and K. Q. Weinberger, Eds. Curran Associates, Inc., 2012, pp. 1097–1105.
- [26] KURAKIN, A., GOODFELLOW, I., AND BENGIO, S. Adversarial examples in the physical world. *arXiv preprint arXiv:1607.02533* (2016).
- [27] LECUN, Y., BENGIO, Y., AND HINTON, G. Deep learning. *nature* 521, 7553 (2015), 436.
- [28] LIN, D., AND STAMP, M. Hunting for undetectable metamorphic viruses, 2011.
- [29] LUONG, M.-T., PHAM, H., AND MANNING, C. D. Effective approaches to attention-based neural machine translation. *arXiv preprint arXiv:1508.04025* (2015).
- [30] MICROSOFT. Kaggle microsoft malware classification challenge. <https://www.kaggle.com/c/malware-classification/data>.
- [31] MIKOLOV, T., CHEN, K., CORRADO, G., AND DEAN, J. Efficient estimation of word representations in vector space. *arXiv preprint arXiv:1301.3781* (2013).
- [32] MOOSAVI DEZFOOLI, S. M., FAWZI, A., AND FROSSARD, P. Deepfool: a simple and accurate method to fool deep neural networks. In *Proceedings of 2016 IEEE Conference on Computer Vision and Pattern Recognition (CVPR)* (2016), no. EPFL-CONF-218057.

- [33] PAPERNOT, N., MCDANIEL, P., GOODFELLOW, I., JHA, S., CELIK, Z. B., AND SWAMI, A. Practical black-box attacks against machine learning. In *Proceedings of the 2017 ACM on Asia Conference on Computer and Communications Security* (2017), ACM, pp. 506–519.
- [34] PAPERNOT, N., MCDANIEL, P., JHA, S., FREDRIKSON, M., CELIK, Z. B., AND SWAMI, A. The limitations of deep learning in adversarial settings. In *Security and Privacy (EuroS&P), 2016 IEEE European Symposium on* (2016), IEEE, pp. 372–387.
- [35] PAPERNOT, N., MCDANIEL, P., WU, X., JHA, S., AND SWAMI, A. Distillation as a defense to adversarial perturbations against deep neural networks. In *Security and Privacy (SP), 2016 IEEE Symposium on* (2016), IEEE, pp. 582–597.
- [36] PENNINGTON, J., SOCHER, R., AND MANNING, C. Glove: Global vectors for word representation. In *Proceedings of the 2014 conference on empirical methods in natural language processing (EMNLP)* (2014), pp. 1532–1543.
- [37] RAFF, E., BARKER, J., SYLVESTER, J., BRANDON, R., CATANZARO, B., AND NICHOLAS, C. Malware Detection by Eating a Whole EXE. *ArXiv e-prints* (Oct. 2017).
- [38] RAFF, E., ZAK, R., COX, R., SYLVESTER, J., YACCI, P., WARD, R., TRACY, A., MCLEAN, M., AND NICHOLAS, C. An investigation of byte n-gram features for malware classification. *Journal of Computer Virology and Hacking Techniques* (2016), 1–20.
- [39] SAMI, A., YADEGARI, B., RAHIMI, H., PEIRAVIAN, N., HASHEMI, S., AND HAMZE, A. Malware detection based on mining api calls. In *Proceedings of the 2010 ACM symposium on applied computing* (2010), ACM, pp. 1020–1025.
- [40] SAXE, J., AND BERLIN, K. Deep neural network based malware detection using two dimensional binary program features. *CoRR abs/1508.03096* (2015).
- [41] SHAHAM, U., ET AL. Understanding adversarial training: Increasing local stability of neural nets through robust optimization. *arXiv preprint arXiv:1511.05432* (2015).
- [42] SHIN, E. C. R., SONG, D., AND MOAZZEZI, R. Recognizing functions in binaries with neural networks. In *24th USENIX Security Symposium (USENIX Security 15)* (Washington, D.C., 2015), USENIX Association, pp. 611–626.
- [43] STOCK, P., AND CISSE, M. Convnets and imagenet beyond accuracy: Explanations, bias detection, adversarial examples and model criticism. *arXiv preprint arXiv:1711.11443* (2017).
- [44] SWIESKOWSKI, P., AND KUZINS, S. Ninite. <https://ninite.com/>.
- [45] SZEGEDY, C., ZAREMBA, W., SUTSKEVER, I., BRUNA, J., ERHAN, D., GOODFELLOW, I., AND FERGUS, R. Intriguing properties of neural networks. *arXiv preprint arXiv:1312.6199* (2013).
- [46] TIELEMAN, T., AND HINTON, G. Lecture 6.5-rmsprop: Divide the gradient by a running average of its recent magnitude. *COURSERA: Neural networks for machine learning 4*, 2 (2012), 26–31.
- [47] VAN DEN OORD, A., DIELEMAN, S., ZEN, H., SIMONYAN, K., VINYALS, O., GRAVES, A., KALCHBRENNER, N., SENIOR, A., AND KAVUKCUOGLU, K. Wavenet: A generative model for raw audio. *arXiv preprint arXiv:1609.03499* (2016).
- [48] XU, W., QI, Y., AND EVANS, D. Automatically evading classifiers. In *Proceedings of the 2016 Network and Distributed Systems Symposium* (2016).
- [49] YUAN, Z., LU, Y., WANG, Z., AND XUE, Y. Droid-sec: deep learning in android malware detection. In *ACM SIGCOMM Computer Communication Review* (2014), vol. 44, ACM, pp. 371–372.